International Journal of Mechanical Sciences 193 (2021) 106181

Contents lists available at ScienceDirect

International Journal of Mechanical Sciences

journal homepage: www.elsevier.com/locate/ijmecsci

Controlling bending deformation of a shape memory alloy-based soft planar gripper to grip deformable objects

Wei Wang [a,*], Yunxi Tang [b,*], Cong Li [c]

[a] Department of Mechanical Engineering, Hanyang University, Seoul 04763, Republic of Korea
[b] Department of Mechanical and Automation Engineering, The Chinese University of Hong Kong, Hong Kong, China
[c] Department of Mechanical Engineering and Materials Science, Duke University, Durham, NC 27708, USA

ARTICLE INFO

Keywords:
Soft grippers
soft robots
smart materials
deformation control

ABSTRACT

Integrating flexible sensors into a soft finger is a common approach to control the deformation of the finger. However, adding sensors, especially sensors with a degree of stiffness, sacrifices the overall compliance of the finger structure and increases the complexity of fabrication and control. This study provides an alternative approach, without the need for integrated sensors, to control the deformation of a shape memory alloy (SMA)-based soft planar gripper for grasping deformable objects. The gripper consists of one soft finger which is an SMA-based hinge actuator capable of producing hinge-like bending deformation. The soft finger can automatically achieve the desired deformation by introducing a closed-loop PID control system. A camera as a vision sensor, instead of integrated flexible sensors, was used to detect the bending deformation of the soft finger in real-time. With the feedback from the camera, the PID controller was implemented in a microcontroller with designed external circuits, to enable the soft finger to reach any targeted bending angle within its deformation range, according to the size of the manipulated object. As a demonstration, the soft planar grippers with the desired deformation were eventually used to grip deformable objects, including flowers and a panicle. Without the need for material characterization and analytical models, the proposed method can also be extended to other soft planar grippers based on different actuation techniques.

1. Introduction

The softness and compliance of flexible structures have been employed by engineers to fabricate soft grippers for adaptive interactions. Compared with their conventional rigid counterparts, soft grippers with a high degree of freedom have shown significant advantages for safely interacting with unpredictable and unconstructed environments, and handling uncertain and dynamic tasks. Soft grippers have been developed with a variety of morphologies, and they can realize the grasping function using different methods including actuation, variable stiffness, and adhesion [1–4]. Among them, soft grippers based on actuation always consist of soft fingers or finger-like components. The deformation of these composed fingers can expand the range of motion of the soft grippers and enable them to perform dexterous grasping.

Grasping an object using a soft fingered gripper can be achieved through both the active deformation of the fingers controlled by the integrated actuators and the further passive adaption to the shape of the object by exploiting the contact. Soft grippers with these characteristics have been developed based on different actuation techniques such as fluidic elastomer actuators [5–10], tendon-driven mechanisms [11–14], electroactive polymers [15–19], shape-memory materials [20–28], particle jamming [29–31], electromagnetic actuation [32–35], and stimuli-responsive polymers and gels [36–42]. Among these techniques, shape memory alloy (SMA)-based soft grippers have shown the advantages of simple and portable configurations, lightweight, simplified actuating methods, and ease of fabrication. However, most of the fingers are designed without deformation control systems, and they are not sensitive to the conditions of contacting the surface between the finger and the gripped object [22,43]. These soft fingers work well for the object with a certain stiffness, which can withstand the force exerted by the fingers without being damaged. However, there remain many challenges for these soft fingers to safely handle deformable objects, due to the deformation control or the lack of sensing to obtain the contact information of the objects.

Integrating stretchable or flexible sensors to the soft grippers is the common approach to enhance the interaction between the grippers and the object being manipulated. These integrated sensors are commonly utilized to indicate strain, force, or pressure for soft robots, and they are usually designed based on resistive or capacitive structures [44–46]. Besides, optical methods have also been developed and implemented in soft grippers [13,47,48]. Although there are various approaches for soft

* Corresponding authors.
E-mail addresses: davidwang@hanyang.ac.kr (W. Wang), tangyunxi000@gmail.com (Y. Tang).

https://doi.org/10.1016/j.ijmecsci.2020.106181
Received 13 July 2020; Received in revised form 9 October 2020; Accepted 30 October 2020
Available online 4 November 2020
0020-7403/

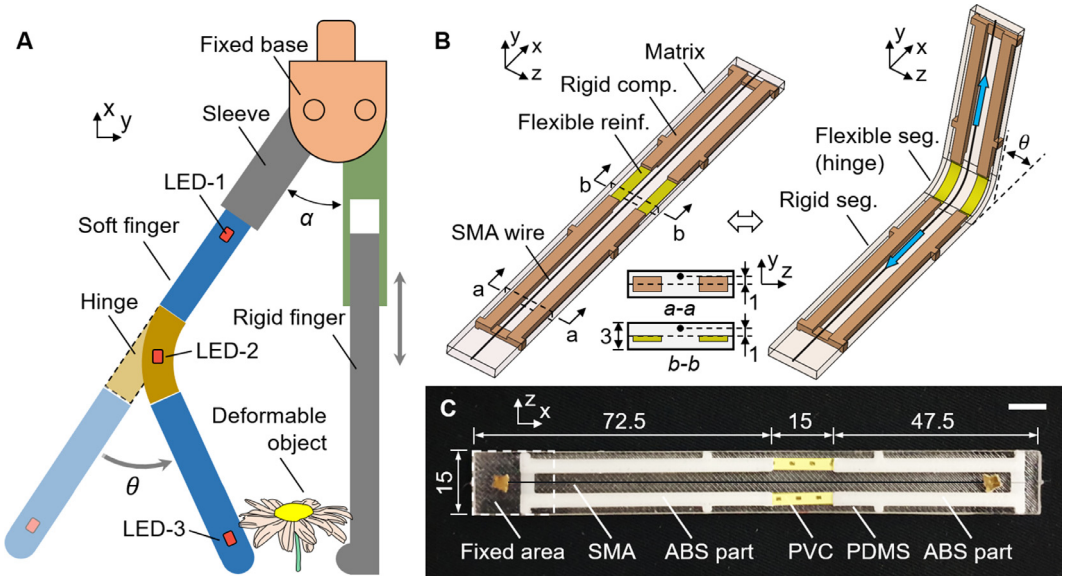

Fig. 1. Configuration of the soft planar gripper. (A) Schematic of the soft gripper consisting of a soft finger and a rigid finger. (B) Schematics of the soft finger actuator before and during actuation. All the components of the actuator are described and the insets show the cross-sections of the actuator at different positions indicating the relative positions of all components. (C) The top view of the fabricated soft finger actuator with all the components and main dimensions. All dimensions are in millimeters and the scale bar is 10 mm.

sensing, it is still challenging to design entirely soft sensors with a large strain [3]. Hence, integrating these sensors, especially the sensors with a certain stiffness, into the soft grippers always increase the stiffness of the finger structure and thus limits the motion of the soft gripper. That is, although adding sensors enables the soft gripper to have certain sensing capabilities, it always sacrifices the overall compliance of the gripper and increases the complexity of fabricating and controlling the soft gripper. Other urgent issues for soft sensors include reliability, robustness, and simple readout [3,49].

This study provides an alternative, a simple and inexpensive approach, without using any integrated sensors, to enable an SMA-based soft planar gripper to achieve the targeted deformation for grasping deformable objects. The soft gripper is composed of two fingers including an SMA-based soft finger being capable of generating pure bending deformation and an immobile rigid finger. The soft finger is able to automatically achieve any targeted bending angles within its deformation range by introducing a closed-loop PID control system mainly composed of image sensing and control circuits. The image sensing, as feedback for the PID controller, is used to calculate the bending angle of the soft finger in real-time. The image sensing was accomplished by using a camera as a vision sensor, instead of using integrated flexible sensors, to capture the bending deformation of the soft finger and transmit the image frames to the computer to calculate the bending angle. The PID controller was implemented in a microcontroller with designed external circuits to enable the soft finger to achieve the targeted deformation, according to the size of the manipulated object. The soft planar gripper with controllable deformation was eventually used to grip deformable objects, including flowers and a panicle.

2. Results and discussion

2.1. Design and working principle of soft planar gripper

The basic design of this study is a soft planar gripper consisting of two fingers, one of which is a soft finger, and the other one is an immobile rigid finger with manually adjustable length attached vertically to the fixed base directly (Fig. 1A). The soft finger is capable of generating hinge-like bending deformation and is inserted in the sleeve and then attached to the fixed base. There is an installed angle α between the two fingers, which is determined so that when the soft finger achieves its maximum bending deformation, the soft gripper can achieve a closed state where the two fingertips contact each other. Three red light-emitting diodes (LEDs) are glued to the side of the soft finger for tracking its bending angle θ. One LED is positioned at the center of the hinge of the soft finger and the other two LEDs are placed on either side of the hinge.

The soft finger is a self-bending hinge actuator fabricated by embedding a pre-strained SMA wire in a flexible matrix with embedded rigid components. The schematic of the actuator with a single hinge and two rigid segments is shown in Fig. 1B. The SMA wire was placed eccentrically from the neutral plane along the length of the actuator. Flexible reinforcements were embedded in the hinge segment to improve the compression resistance and bending recovery ability of the hinge segment. The schematics of the cross-sections of the actuator *a-a* of the rigid segment and *b-b* of the flexible segment are shown in the insets of Fig. 2B, indicating the layout of the components including the eccentric distance 1mm of the SMA wire to the geometrical middle plane. Applying an electric current to the pre-strained SMA wire causes its temperature to increase to its austenite phase transition temperature through Joule heating. The eccentrically embedded SMA wire will start to contract in the matrix to generate a bending moment, which enables the actuator to produce a bending deformation concentrated on the hinge segment, while the rigid segment with greater stiffness cannot bend [22,50]. After removing the electrical current, the SMA wire cools down below its austenite phase transition temperature through heat dissipation, the actuator begins to recover to its original flat shape by exploiting stored bending energy of the deformed hinge segment. This process can be repeated by applying and removing the electrical current. The configurations of the actuator before and during actuation, with a bending angle θ, are shown on the left and right sides of Fig. 1B.

2.2. Fabrication of soft planar gripper

The main component of the soft planar manipulator is the soft finger which is composed of smart materials, a flexible matrix, and an embedded, rigid structure. In this study, SMA wire is used as the smart material for actuation, polydimethylsiloxane (PDMS) elastomer as the flexible matrix, polyvinyl chloride (PVC) plate as the flexible reinforce-

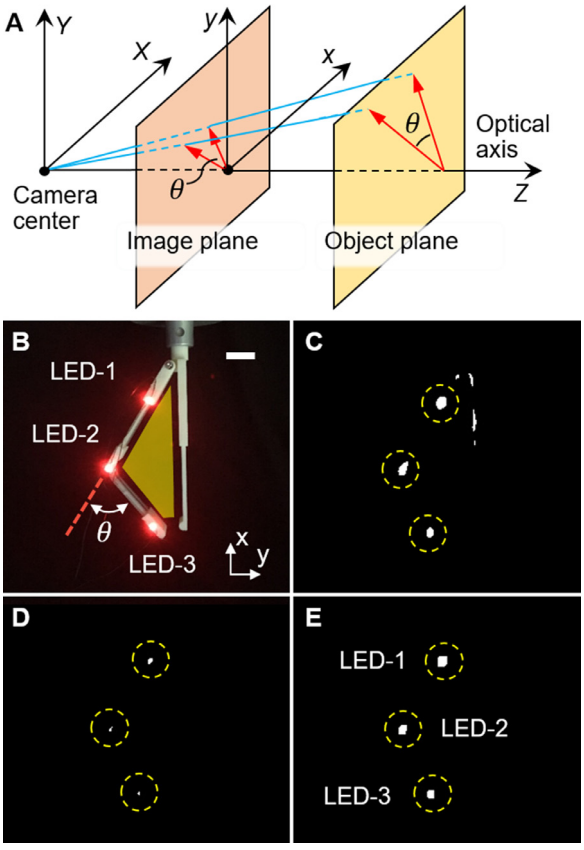

Fig. 2. Image processing for the measurement of the bending angle. (A) Schematic of the central projection model of the camera when the object plane is parallel to the image plane. A mirror image is formed behind the camera center, while a virtual image plane is depicted in front of the camera center. (B) Original RGB image of the actuated gripper. The enclosed area formed between the two fingers is indicated in yellow. The RGB image is converted to the HSV image to find the positions of the three LEDs, with the steps of choosing red channel (C), the erode operation (D), and the dilate operation (E). The positions of LEDs are indicated in dashed yellow circles. The scale bar is 20 mm.

ment, and acrylonitrile butadiene styrene (ABS) for fabricating the embedded rigid components and some auxiliary parts and molds, and all materials used are commercially available.

It is difficult to fabricate a soft finger composed of different functional components, especially for the unprintable SMA wire, in a single step, therefore, the soft finger was fabricated utilizing rapid and adaptable fabrication approaches including materials molding process and 3D printing. The first step to fabricate the soft finger actuator was to use a 3D printer (Dimension 768 SST, Stratasys) to fabricate an ABS mold with small holes for positioning the SMA wire within the matrix. Then, the SMA wire (Ni-Ti, 55-45 wt.%, Dynalloy) with a diameter of 0.15 mm was placed in the mold by inserting it through the small holes, pre-strained, and fixed to a jig. The rigid components were built using the same printer, and the PVC plate with a thickness of 0.2 mm was laser cut (M-300, Universal Laser Systems) into small rectangular pieces, which were then glued to the two rigid components to form an embedded integrated structure. The structure was then placed at the bottom of the mold. After that, PDMS (Sylgard 184, Dow Corning) was mixed with a 10:1 ratio to the curing agent, degassed in a vacuum pump, poured into the mold, and then the assembly was cured for 8 h at 55°C, which is below the actuation temperature of the SMA wire. After the curing process and removing the mold, the fabricated finger actuator was obtained and its main dimensions are described in Fig. 1C. The overall dimensions of the finger actuator are 135 × 15 × 3 mm (length × width × thickness) where the hinge segment is 15 mm long and 47.5 mm from the fingertip.

The fixed base, sleeve, and rigid finger were built using the same 3D printer. There is a small protrusion on the inside of the fingertip of the rigid finger to prevent the object from falling when grasped. After the fabrication of all components, the soft planar manipulator was assembled by first inserting the soft finger into a sleeve, and then two fingers were mounted to the fixed base using revolute joints. After assembling, three LEDs were then attached to one side of the soft finger.

2.3. Bending angle measurement using image processing

The soft gripper contains one soft finger, so the deformation of the finger can be regarded as the deformation of the gripper. Without integrated sensors inside the soft finger, a camera as a vision sensor was used to track the bending deformation of the soft finger. Considering the gripper is planar, only one monocular camera is needed, provided that the plane of the soft finger should be parallel with the image plane such that the bending angle is unchanged during projective transformation, as shown in Fig. 2A. The geometric explanation in the figure shows the bending angle of the soft finger in the object plane is identically equal to the angle displayed in the image plane. Three red LEDs as marks are attached to one side of the soft finger so that the bending angle can be determined as the acute angle θ between the line connecting the LED-1 and LED-2 and the line connecting the LED-2 and LED-3 (Fig. 2B).

A cellphone camera was utilized in this study to capture the varying deformation of the soft finger upon actuation by recording image frames at a rate of 30 fps in real-time, enabling the image sequence with a fixed time interval of 0.1 s to be obtained from the live camera. The image frames were transmitted to the computer, and then the measurement of soft finger deformation was automatically completed for each image frame through an image processing program developed using Python (version 3.7). In order to detect the relative positions of the three LEDs in the image, the image in red-green-blue (RGB) format (Fig. 2B) was converted to the hue-saturation-value (HSV) format to extract the red tunnel of the original RGB image. The corresponding thresholds for hue, saturation, and value were determined as 0 and 16, 0 and 44, and, 200 and 255, respectively. The extracted image was then converted to a binary image so that the regions (bright regions) of the three LED markers can be obtained (Fig. 2C).

These obtained regions are irregular and noisy, which even involve some unmarked extra bright regions. Next, the morphological operators including erosion and dilation were used to remove the noise and patches. In the erode operation, a binary structuring element S, which is a 3 × 3 pixel box, was selected, assuming the origin of S is located at its center. Each pixel in Fig. 2C was superimposed by the origin of S, and then the minimum value overlapping with S can be found. The image was then eroded by replacing the current image using the minimum value (Fig. 2D). In the dilate operation, another binary structuring element S' of a 5 × 5 pixel box was chosen with the origin at the center, and the eroded image was scanned by S'. Then, calculating the maximal value overlapped by S' and replacing the image pixel in the anchor point with maximal value to obtain the dilated image that clearly shows the positions of the three LEDs (Fig. 2E). The bending angle θ of the soft finger can be then analyzed in virtue of the extracted positions of the three LEDs based on the triangle cosine theorem.

2.4. Characterization of bending deformation of soft finger

The hinge-like deformation of the soft finger can be achieved by applying an electrical current to the two ends of the embedded SMA wire. The maximum value of the current that causes the maximum deformation was determined as 0.6 A with a corresponding applied voltage of 9.2 V through trial-and-error to allow for the sustained actuation and preventing overheating of the SMA wire (left inset of Fig. 3A, Movie S1). A microcontroller, Arduino Uno board was used to trigger the bending deformation of the soft finger through a designed drive circuit to provide enough power and to control the applied current to the SMA wire.

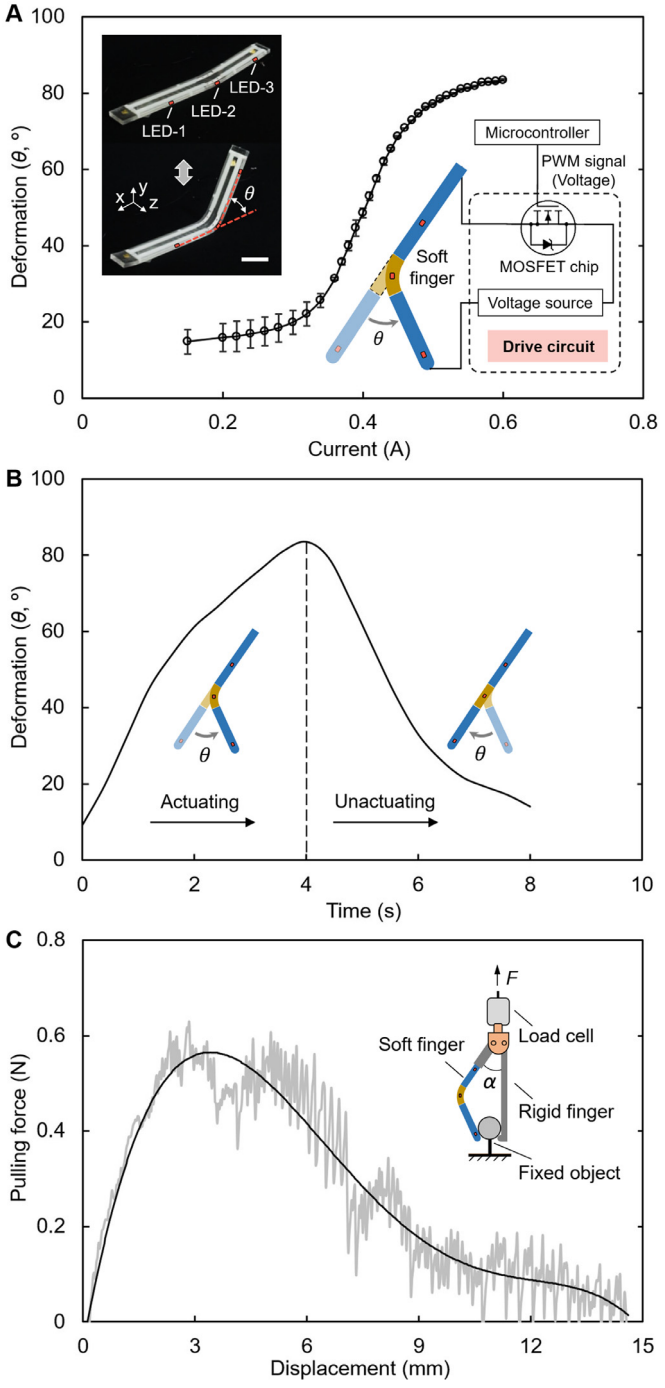

Fig. 3. Characterization of bending deformation of the soft finger. (A) Effect of different applied currents on the maximum bending deformation of the finger actuator. The left inset shows the configurations of the soft finger before and during actuation, and the right inset shows the schematic of the control circuit. Scale bar is 20 mm. (B) Time for the soft finger actuator to reach its maximum bending deformation with a directly applied current of 0.6 A, and time to restore its shape after removing the current. Insets show the schematics of the deformation of the finger actuator. (C) Pulling force of the gripper from caging the fixed cylindric object to its separation. The inset shows the schematic of the experimental setup.

The key electrical component of the drive circuit is the metal-oxide-semiconductor field-effect transistor (MOSFET). The Arduino Uno board was programmed to generate a proper pulse width modulation (PWM) signal which is the voltage value to be used as the input gate voltage of the MOSFET. The driving circuit mainly adopts the MOSFET component to change the magnitude of the applied current to SMA wire controlled by the PWM signal, and the schematic of the circuit is illustrated in the inset of Fig. 2A. Under a constant voltage of 9.2 V provided by the voltage source, the current applied to the SMA wire can be changed by applying PWM waves with different duty cycles to the gate electrode (right inset of Fig. 3A).

In order to determine the bending deformation θ, electrical currents of 0.15 A, ranging from 0.2 A to 0.4 A in increments of 0.02 A, and ranging from 0.4 A to 0.6 A in increments of 0.01 A, were applied to the finger actuator through the drive circuit, and the final bending deformation is measured using the image processing method. The results for the maximum bending angle with different applied currents are shown in Fig. 3. It shows that there is a one-to-one correlation between the applied current and the amount of deformation, which is related to the induced fraction of the crystal phase transformation from martensite to austenite in the SMA wire. It can also be seen from the figure that the deformation undergoes three stages. In the first stage, for currents between 0.15 A and 0.34 A, the deformation gradually increases as the current increases. In the second stage, for currents between 0.34 A and 0.47 A, the deformation rapidly increases as the current increases. For currents larger than 0.47 A, the deformation slowly approaches the maximum bending angle, and the maximum current of 0.6 A enables the finger to achieve a maximum bending deformation of 83.5°. The actuating speed of the soft finger to reach its maximum bending deformation with a directly applied current of 0.6 A and the recovery speed to restore its shape after removing the current are measured (Fig. 3B). The result shows that it takes about 4 s for the soft finger to reach its maximum deformation, and around 4 s to restore its shape. Besides, it can be seen that there is a slight initial deformation of around 9° for the soft finger before actuation, which is caused by the eccentrically embedded prestrained SMA wire. In addition, the actuation speed of the soft finger can be improved by using multiple thinner SMA wires to replace the embedded one thicker SMA wire and the recovery speed can be accelerated by introducing cooling systems [30,31]. However, these approaches will increase the complexity of manufacturing and control, which are not considered in this work.

The corresponding installed angle α between these two fingers of the gripper was then experimentally determined as around 34° with a maximum bending deformation of the soft finger of 83.5°. The gripper with the installed angle between two fingers of 34° is installed to a load cell to measure the force generated by the gripper on a fixed object during an upward movement. The measurement starts by placing the gripper to execute a fully grasping with the applied current of 0.6 A on a fixed cylindrical object with a diameter of 30 mm, as shown in the inset of Fig. 3C. The gripper is then moved upwards and the actuated soft finger passively adapts its deformed shape according to the contour of the object. During this process, the vertical pulling force generated by the gripper on the object is shown in Fig. 3C. One can see from the curve that the pulling force first increases fast and then gradually decreases, depending on the contacting position between the fingers of the gripper and the spherical surface, and the maximum grasping force of the gripper is around 0.57 N.

2.5. Bending deformation control

The image processing and driving circuits are integrated with the addition of peripheral equipment. This constructs a closed-loop PID control system to enable the soft finger to automatically achieve the targeted bending angle according to the size of the picked object. The overall control architecture is described in Fig. 4A. The workflow of the PID control system includes: 1) collecting real-time bending angles from the

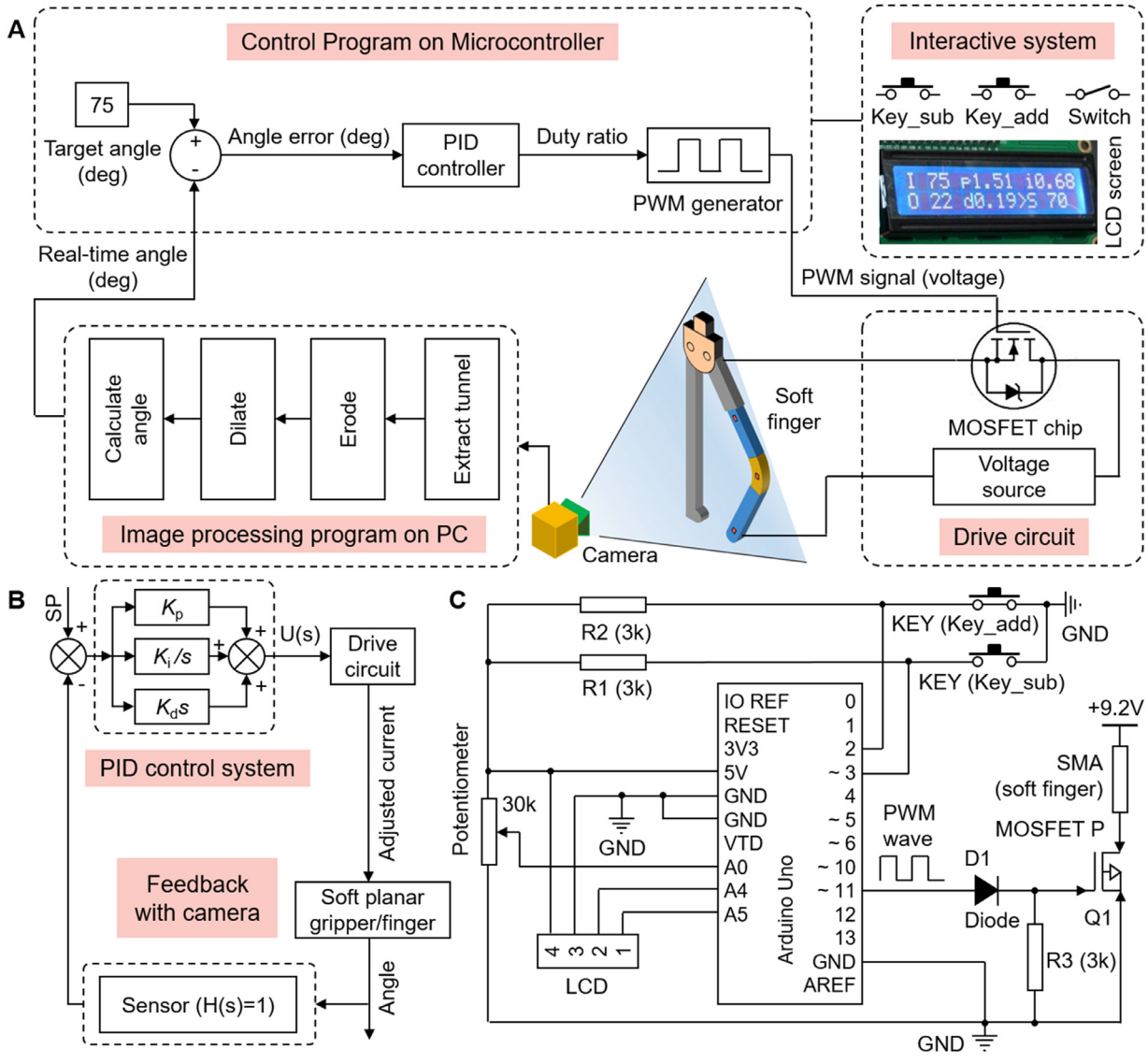

Fig. 4. Schematic diagrams of the control system. (A) The overall architecture of the controller consisting of three main parts including image sensing to detect the bending deformation of the soft finger in real-time, PID controller implemented in a microcontroller to enable the soft finger to reach any targeted bending angles, and peripheral equipment. (B) Flow chart of the PID control system. (C) Schematic of the designed circuit including drive circuit and peripheral equipment.

image processing program, 2) calculating the duty cycle value of the PWM signal for the drive circuit, based on the angle error between the current and target bending angle, and 3) adjusting the current applied to the finger by generating a PWM signal based on the new duty cycle value and sending to the drive circuit. The flow chart of the PID control system is shown in Fig. 4B. The setpoint is a predefined target bending angle determined by the size of the picked object. U(s) is the output control signal of the PID controller. The discrete form of the PID algorithm is shown below

$$u(k) = K_P e(k) + K_i \sum_{j=0}^{k} e(j) + K_d(e(k) - e(k-1))$$

where k is the k-th time step, p_{target} is the targeted bending angle, $e(k) = p(k) - p_{\text{target}}$ is the deformation error, and $u(k)$ is the control signal. The PID controller consists of three terms, including proportional term $K_p e(k)$ being able to counteract the effect of interference quickly, the integral term $K_i \sum_{j=0}^{k} e(j)$ to eliminate static errors, and differential term $K_d(e(k) - e(k-1))$ to improve the rapidity of the system response.

The PID controller was implemented in the microcontroller and the schematic of the designed circuit for the system is shown in Fig. 4C. The output control signal U(s) is the voltage of the analog pin of A11, which actually is the duty cycle of PWM to be used as the input voltage of the drive circuit for the soft finger. A diode is connected to pin A11 to prevent current from flowing back and damaging the chip. Under a voltage of 9.2 V provided by the voltage source, the current through the SMA wire can be changed by applying PWM waves with different duty cycles on the gate electrode of the MOSFET. For interactive system part, the potentiometer can change the measured voltage V_{A0} of pin A_0 by tuning its resistance so that the selection indicator (an arrow) for different parameters shown on the LCD screen will move according to V_{A0}. All the parameters, including K_p, K_d, K_i, and p_{target} stored in EEPROM of Arduino, can then be manually tuned once an interrupt was triggered. The interrupt was achieved by pressing down the keys of *Key_add* and *Key_sub* to reduce the voltages of pin 2 and pin 3 to 0. The LCD module is used to display the relative parameters and to monitor how the bending angle in real-time is changing. The symbols of I, p, i, O, d, S, and > on the screen indicate the real-time bending angle, proportional term, integral term, PWM signal (with the current duty cycle of 22/255),

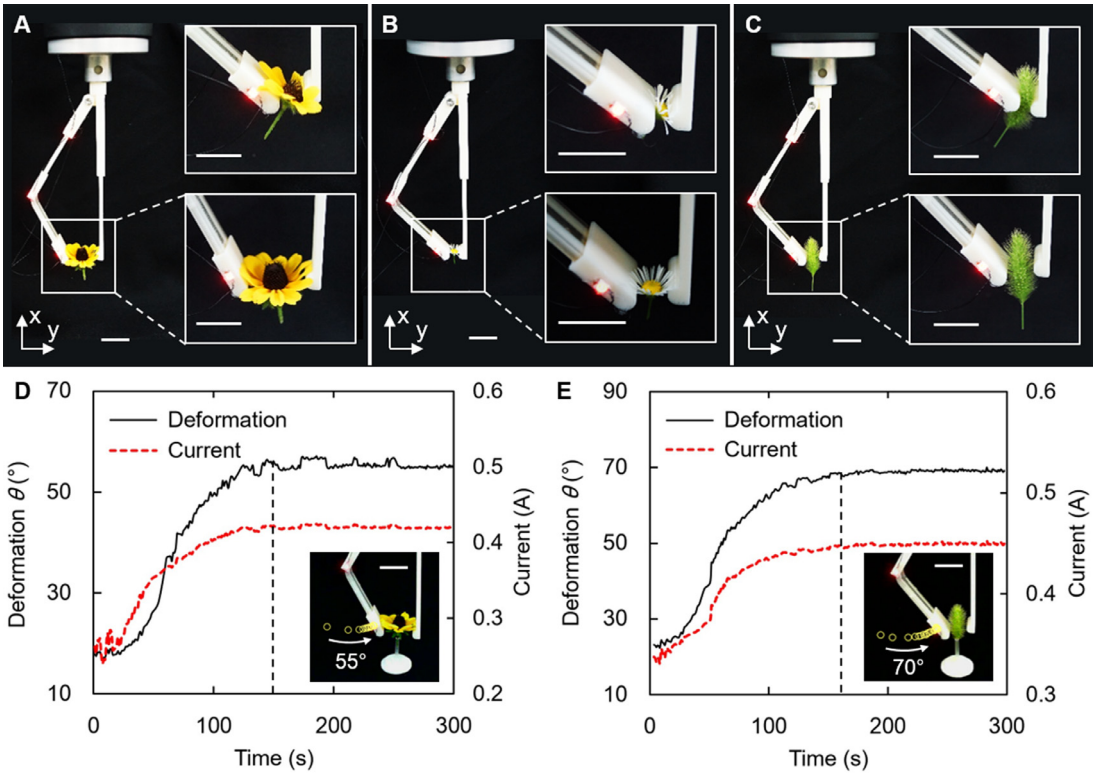

Fig. 5. Evaluation of grasping performance. The gripper is utilized to grip two daisy-like flowers with different sizes (A, B) and a panicle of green bristlegrass (C). The upper-right and bottom-left insets show the grasping performance with the open-loop and closed-loop control systems, respectively. A 55-degree and 70-degree targeted deformation of the soft finger is utilized to grip the daisy-like flower (D) and the panicle (E) respectively, as shown in the insets where the trajectory of the soft fingertip is indicated using small yellow circles. All scale bars are 20 mm.

derivative term, targeted bending angle, and selection indicator, respectively.

2.6. Evaluation of grasping performance

Position and force control is usually the main concern for manipulator operation. The main task of the soft gripper in this study is to grasp some deformable and lightweight objects with lower stiffness and less contact force compared with traditional rigid manipulators. Therefore, there are low requirements on the force control of the designed soft gripper and it is reasonable to perform position control here to ensure reliable contact between the gripper and the objects. In order to test the accuracy and stability of the control system in meeting a target value of the bending angle of the soft finger, a series of experiments of the gripper was conducted, in which values of target angles of the finger were input to the controller, to grip delicate objects with determined size. The maximum size of the object to be grasped is determined as around 40 mm mainly depending on the maximum transverse width of the enclosed area formed between the two fingers with an installed angle of 34°, as shown in Fig. 2B. An object with a larger size can be grasped through enlarging the enclosed area formed between the two fingers by using fingers with longer length or increasing the installed angle between the two fingers. This research aims to enable the soft finger to achieve a controllable bending deformation through active control strategies. Hence, the automatic recognition of the position and size of objects is not considered in this research. The gripper was utilized to grip the fragile and deformable structures, including two daisy-like flowers and a panicle of green bristlegrass with different contour diameters of around 26 mm, 10 mm, and 10 mm, respectively. The objects were initially placed close to the rigid finger so the soft finger can reach them by the sequential bending deformation. In order to stably grasp the objects without damage, the bending angles of the soft finger were experimentally predetermined as 70° to grip the daisy-like flower with a greater diameter, and 55° to grip the flower with a smaller diameter and the panicle.

The experiments were first conducted with an open-loop control system. A constant electrical current of 0.6 A is directly applied to the embedded SMA wire in the soft finger using a power supply, and the soft finger can generate the maximum bending angle (83.5°) to enable the gripper to reach a closed state without holding anything. When grasping, it can be seen that the flowers and panicle are severely squeezed and damaged by the soft finger (upper-right insets of Fig. 5A-C), since the objects are ultra-soft and their stiffness cannot stand the bending force of the soft finger.

In the next experiments, the control loop was closed with PID controller, and the gripper can generate the target bending angles to pick up the flowers (70° and 55°) by holding its petals and to pick up the panicle (55°) by holding its bristles (Fig. 5A-C, Movie S2). Figures 5D and 5E describe the trend of the bending angle of the soft finger and the corresponding applied driving current to achieve the target angles of 70° and 55°. It can be seen that it will take around 150 s and 170 s for the control system to enable the soft finger to achieve the final stable bending angles of 55° and 70°, corresponding to the final stable currents of 0.42 A and 0.46 A, respectively (Fig. 5D, 5E). The position of the soft fingertip (i.e. the position of LED-3) during grasping is tracked every 20 s using a video analysis tool and the trajectory is shown in the insets of Fig. 5D-E. It can be seen that the soft finger can smoothly and stably approach the target angles. Moreover, it is possible to reduce the needed time to reach the target angle by applying a larger current close to the maximum stable current from the beginning. The experimental results show that the soft finger can reach a stable bending deformation to grip the objects successfully. The system response is not fast due to the characteristic of SMA and it will be difficult to track a high-speed trajectory for the gripper with the current design. However, the soft gripper with a simple structure can still con-

duct many low-speed grasping tasks easily and cause less damage to objects.

3. Conclusion

This work demonstrated an approach of controlling the bending angle of a soft finger for a planar gripper being capable of grasping delicate and deformable objects. The soft finger is an SMA-based hinge actuator capable of pure bending deformation concentrated on the hinge section of the actuator. The soft finger was able to automatically achieve the desired deformation by introducing a closed-loop PID control system mainly consisting of image sensing and control circuits. A cellphone camera as a vision sensor, instead of integrated flexible sensors, was used to detect the bending deformation of the soft finger in real-time. Utilizing the detected deformation as the feedback, a PID controller was implemented in a microcontroller with designed external circuits, to enable the soft finger to reach any targeted bending angles within its deformation range according to the size of the manipulated object. The soft gripper with controllable deformation was finally used to grip different deformable objects.

Without flexible sensors attached to or embedded in the soft finger, it is possible to maintain the overall compliance of the finger structure and reducing the complexity of the fabrication process. Although various methods for controlling SMA wires have been studied in previous research, this work provides a strategy for controlling SMA-based soft planar gripper using a PID control system to enable the composed soft finger to achieve any targeted bending angle within its deformation range. The choice of using SMA-based actuation was motived mainly by the fact that such actuators are easy to fabricate in a portable configuration, can be easily actuated, and can generate reasonable deformation. In addition, this proposed approach avoids the need for material characterization and analytical models for the soft finger that could be difficult to achieve in some cases and is not constrained to a specific actuating principle, which can be extended to other soft planar grippers based on different actuation techniques.

The automatic recognition of the size of objects is not studied in this work which will be considered in future work. The convex hull will be utilized to approximate the edge shape of the object and to find the maximum transverse width in the image plane. The maximum transverse width will be converted to the world coordinate using the transform matrix of a calibrated camera. Then the soft finger will generate the required bending deformation according to the coordinate. Other future works include improving the control system to accelerate the response speed of the soft finger and implementing control of soft grippers in three-dimensional space.

Declaration of Competing Interest

The authors declare that they have no known competing financial interests or personal relationships that could have appeared to influence the work reported in this paper.

.

CRediT authorship contribution statement

Wei Wang: Conceptualization, Methodology, Supervision, Writing - review & editing. **Yunxi Tang:** Methodology, Software, Data curation, Writing - original draft. **Cong Li:** Methodology, Software, Data curation.

Acknowledgments

This work was supported by the National Research Foundation of Korea (NRF) grant funded by the Korea government (MSIT) (No.2020R1C1C1010295), (MSIT) (No.2019R1F1A1062619), and by the research fund of Hanyang University (HY-2019). The authors would like to thank the reviewers for their insightful feedback.

Supplementary materials

Supplementary material associated with this article can be found, in the online version, at doi:10.1016/j.ijmecsci.2020.106181.

References

[1] Tonazzini A, Mintchev S, Schubert B, Mazzolai B, Shintake J, Floreano D. Variable Stiffness Fiber with Self-Healing Capability. Adv Mater 2016:10142–8.
[2] Amend J, Lipson H. The JamHand: Dexterous Manipulation with Minimal Actuation. Soft Robot 2017;4:70–80.
[3] Hughes J, Culha U, Giardina F, Günther F, Rosendo A. Soft Manipulators and Grippers: A Review. Front Robot AI 2016;3:1–12.
[4] Manti M, Cacucciolo V, Cianchetti M. Stiffening in Soft Robotics: A Review of the State of the Art. IEEE Robot Autom Mag 2016;23:93–106.
[5] Gorissen B, Reynaerts D, Konishi S, Yoshida K, Kim JW, De Volder M. Elastic Inflatable Actuators for Soft Robotic Applications. Adv Mater 2017;29:1–14.
[6] Deimel R, Brock O. A novel type of compliant and underactuated robotic hand for dexterous grasping. Int J Rob Res 2016;35:161–85.
[7] Sinatra NR, Teeple CB, Vogt DM, Parker KK, Gruber DF, Wood RJ. Ultragentle manipulation of delicate structures using a soft robotic gripper. Sci Robot 2019;4:eaax5425.
[8] Zhong G, Hou Y, and Dou W. A soft pneumatic dexterous gripper with convertible grasping modes. Int J Mech Sci 2019;153: 445-456.
[9] Lee JG, Rodrigue H. Efficiency of Origami-Based Vacuum Pneumatic Artificial Muscle for Off-Grid Operation. Int J Precis Eng Manuf - Green Technol 2019;6:789–97.
[10] Schaffner M, Faber JA, Pianegonda L, Rühs PA, Coulter F, Studart AR. 3D printing of robotic soft actuators with programmable bioinspired architectures. Nat Commun 2018;9:878.
[11] Lee J-H, Chung YS, Rodrigue H. Long Shape Memory Alloy Tendon-based Soft Robotic Actuators and Implementation as a Soft Gripper. Sci Rep 2019;9:1–12.
[12] Manti M, Hassan T, Passetti G, D'Elia N, Laschi C, Cianchetti M. A Bioinspired Soft Robotic Gripper for Adaptable and Effective Grasping. Soft Robot 2015;2:107–16.
[13] Odhner LU, Jentoft LP, Claffee MR, Corson N, Tenzer Y, Ma RR, et al. A compliant, underactuated hand for robust manipulation. Int J Rob Res 2014;33:736–52.
[14] Kang BB, Choi H, Lee H, Cho K-J. Exo-Glove Poly II: A Polymer-Based Soft Wearable Robot for the Hand with a Tendon-Driven Actuation System. Soft Robot 2018;00:soro.2018.0006.
[15] Shintake J, Rosset S, Schubert B, Floreano D, Shea H. Versatile Soft Grippers with Intrinsic Electroadhesion Based on Multifunctional Polymer Actuators. Adv Mater 2016;28:231–8.
[16] Lau GK, Heng KR, Ahmed AS, Shrestha M. Dielectric elastomer fingers for versatile grasping and nimble pinching. Appl Phys Lett 2017;110:182906.
[17] Shian S, Bertoldi K, Clarke DR. Dielectric Elastomer Based "grippers" for Soft Robotics. Adv Mater 2015;27:6814–9.
[18] Duduta M, Hajiesmaili E, Zhao H, Wood RJ, Clarke DR. Realizing the potential of dielectric elastomer artificial muscles. Proc Natl Acad Sci U S A 2019;116:2476–81.
[19] Kim SJ, Kim O, Park MJ. True Low-Power Self-Locking Soft Actuators. Adv Mater 2018;30:1–7.
[20] Won P, Park JJ, Lee T, Ha I, Han S, Choi M, et al. Stretchable and Transparent Kirigami Conductor of Nanowire Percolation Network for Electronic Skin Applications. Nano Lett 2019;19:6087–96.
[21] Wang W, Li C, Cho M, Ahn S-H. Soft Tendril-Inspired Grippers: Shape Morphing of Programmable Polymer–Paper Bilayer Composites. ACS Appl Mater Interfaces 2018;10:10419–27.
[22] Wang W, Rodrigue H, Kim H-I, Han M-W, Ahn S-H. Soft composite hinge actuator and application to compliant robotic gripper. Compos Part B Eng 2016;98:397–405.
[23] Wang W, Ahn S-H. Shape Memory Alloy-Based Soft Gripper with Variable Stiffness for Compliant and Effective Grasping. Soft Robot 2017:soro.2016.0081.
[24] Engeberg ED, Dilibal S, Vatani M, Choi J-W, Lavery J. Anthropomorphic finger antagonistically actuated by SMA plates. Bioinspir Biomim 2015;10:056002..
[25] Wang W. Mechanical Assembly of Thermo-Responsive Polymer-Based Untethered Shape-Morphing Structures. Macromol Mater Eng 2020;305:1900568.
[26] Kim H Il, Han MW, Song SH, Ahn SH. Soft morphing hand driven by SMA tendon wire. Compos Part B Eng 2016;105:138–48.
[27] Rodrigue H, Wang W, Kim D-R, Ahn S-H. Curved Shape Memory Alloy-based Soft Actuators and Application to Soft Gripper. Compos Struct 2017;176:398–406.
[28] Rodrigue H, Wang W, Han M-W, Kim TJY, Ahn S-H. An Overview of Shape Memory Alloy-Coupled Actuators and Robots. Soft Robot 2017;4:soro.2016.0008.
[29] Licht S, Collins E, Mendes ML, Baxter C. Stronger at Depth: Jamming Grippers as Deep Sea Sampling Tools. Soft Robot 2017;4:305–16.
[30] Brown E, Rodenberg N, Amend J, Mozeika A, Steltz E, Zakin MR, et al. Universal robotic gripper based on the jamming of granular material. Proc Natl Acad Sci 2010;107:18809–14.
[31] Yang Y, Zhang Y, Kan Z, Zeng J. Hybrid Jamming for Bioinspired Soft Robotic Fingers. Soft Robot 2020;7:292–308.
[32] Do TN, Phan H, Nguyen TQ, Visell Y. Miniature Soft Electromagnetic Actuators for Robotic Applications. Adv Funct Mater 2018;28:1800244.
[33] Mirvakili SM, Sim D, Hunter IW, Langer R. Actuation of untethered pneumatic artificial muscles and soft robots using magnetically induced liquid-to-gas phase transitions. Sci Robot 2020;5:eaaz4239.
[34] Ren Z, Hu W, Dong X, Sitti M. Multi-functional soft-bodied jellyfish-like swimming. Nat Commun 2019;10:2703.
[35] Kim Y, Parada GA, Liu S, Zhao X. Ferromagnetic soft continuum robots. Sci Robot 2019;7329:1–16.

[36] Kobayashi K, Yoon C, Oh SH, Pagaduan J V., Gracias DH. Biodegradable Thermomagnetically Responsive Soft Untethered Grippers. ACS Appl Mater Interfaces 2019;11:151–9.
[37] Li M, Jiang Z, An N, Zhou J. Harnessing programmed holes in hydrogel bilayers to design soft self-folding machines. Int J Mech Sci 2018;140: 271-278.
[38] Zheng SY, Shen Y, Zhu F, Yin J, Qian J, Fu J, et al. Programmed Deformations of 3D-Printed Tough Physical Hydrogels with High Response Speed and Large Output Force. Adv Funct Mater 2018;1803366:1803366.
[39] Ongaro F, Scheggi S, Yoon CK, van den Brink F, Oh SH, Gracias DH, et al. Autonomous planning and control of soft untethered grippers in unstructured environments. J Micro-Bio Robot 2017;12:45–52.
[40] He Q, Wang Z, Wang Y, Minori A, Tolley MT, Cai S. Electrically controlled liquid crystal elastomer-based soft tubular actuator with multimodal actuation. Sci Adv 2019;5:eaax5746.
[41] Yum K, Jeon J, Nojoomi A, Arslan H. 3D Printing of Anisotropic Hydrogels with Bioinspired Motion. Adv Sci 2018;1800703.
[42] Ji Z, Yan C, Yu B, Zhang X, Cai M, Jia X, et al. 3D Printing of Hydrogel Architectures with Complex and Controllable Shape Deformation. Adv Mater Technol 2019;1800713:1–8.
[43] Wang W, Yu CY, Abrego Serrano PA, Ahn S-H. Shape Memory Alloy-Based Soft Finger with Changeable Bending Length Using Targeted Variable Stiffness. Soft Robot 2020;7:283–91.
[44] Koivikko A, Raei ES, Mosallaei M, Mäntysalo M, Sariola V. Screen-printed curvature sensors for soft robots. IEEE Sens J 2018;18:223–30.
[45] Elgeneidy K, Lohse N, Jackson M. Bending angle prediction and control of soft pneumatic actuators with embedded flex sensors - A data-driven approach. Mechatronics 2018;50:234–47.
[46] Tavakoli M, Lopes P, Lourenço J, Rocha RP, Giliberto L, De Almeida AT, et al. Autonomous Selection of Closing Posture of a Robotic Hand Through Embodied Soft Matter Capacitive Sensors. IEEE Sens J 2017;17:5669–77.
[47] Zhao H, O'Brien K, Li S, Shepherd R. Optoelectronically Innervated Soft Prosthetic Hand via Stretchable Optical Waveguides. Sci Robot 2016;7529:1–10.
[48] Heo JS, Kim KY, Lee JJ. Development of a distributed force detectable artificial skin using microbending optical fiber sensors. J Intell Mater Syst Struct 2009;20:2029–36.
[49] Polygerinos P, Correll N, Morin SA, Mosadegh B, Onal CD, Petersen K, et al. Review of Fluid-Driven Intrinsically Soft Devices: Manufacturing, Sensing, Control, and Applications in Human-Robot Interaction. Adv Eng Mater 2017;19:1700016.
[50] Wang W, Kim N-G, Rodrigue H, Ahn S-H. Modular assembly of soft deployable structures and robots. Mater Horiz 2017;4:367–76.